Available online at www.sciencedirect.com
SCIENCE DIRECT®
Biomaterials 27 (2006) 519–533
Biomaterials
www.elsevier.com/locate/biomaterials

Matrix inclusion within synthetic hydrogel guidance channels improves specific supraspinal and local axonal regeneration after complete spinal cord transection

Eve C. Tsai[a], Paul D. Dalton[b], Molly S. Shoichet[b,*], Charles H. Tator[a,**]

[a]*Toronto Western Hospital Research Institute and Krembil Neuroscience Centre, University of Toronto, Toronto Western Research Institute, Toronto Western Hospital, Room 12-423, McLaughlin Wing, 399 Bathurst St., Toronto, Ontario, Canada M5T 2S8*
[b]*Department of Chemical Engineering & Applied Chemistry, Department of Chemistry, Institute of Biomaterials and Biomedical Engineering, University of Toronto, 4 Taddle Creek Road, Room 407, Toronto, ON M5S 3G9*

Received 6 July 2005; accepted 12 July 2005
Available online 11 August 2005

Abstract

We have previously shown that a novel synthetic hydrogel channel composed of poly(2-hydroxyethyl methacrylate-*co*-methyl methacrylate) (pHEMA-MMA) is biocompatible and supports axonal regeneration after spinal cord injury. Our goal was to improve the number and type of regenerated axons within the spinal cord through the addition of different matrices and growth factors incorporated within the lumen of the channel. After complete spinal cord transection at T8, pHEMA-MMA channels, having an elastic modulus of 263 ± 13 kPa were implanted into adult Sprague Dawley rats. The channels were then filled with one of the following matrices: collagen, fibrin, Matrigel™, methylcellulose, or smaller pHEMA-MMA tubes placed within a larger pHEMA-MMA channel (called tubes within channels, TWC). We also supplemented selected matrices (collagen and fibrin) with neurotrophic factors, fibroblast growth factor-1 (FGF-1) and neurotrophin-3 (NT-3). After channel implantation, fibrin glue was applied to the cord-channel interface, and a duraplasty was performed with an expanded polytetrafluoroethylene (ePTFE®) membrane. Controls included animals that had either complete spinal cord transection and implantation of unfilled pHEMA-MMA channels or complete spinal cord transection. Regeneration was assessed by retrograde axonal tracing with Fluoro-Gold, and immunohistochemistry with NF-200 (for total axon counts) and calcitonin gene related peptide (CGRP, for sensory axon counts) after 8 weeks survival. Fibrin, Matrigel™, methylcellulose, collagen with FGF-1, collagen with NT-3, fibrin with FGF-1, and fibrin with NT-3 increased the total axon density within the channel (ANOVA, $p < 0.05$) compared to unfilled channel controls. Only fibrin with FGF-1 decreased the sensory axon density compared to unfilled channel controls (ANOVA, $p < 0.05$). Fibrin promoted the greatest axonal regeneration from reticular neurons, and methylcellulose promoted the greatest regeneration from vestibular and red nucleus neurons. With Matrigel™, there was no axonal regeneration from brainstem motor neurons. The addition of FGF-1 increased the axonal regeneration of vestibular neurons, and the addition of NT-3 decreased the total number of axons regenerating from brainstem neurons. The fibrin and TWC showed a consistent improvement in locomotor function at both 7 and 8 weeks. Thus, the present study shows that the presence and type of matrix contained within synthetic hydrogel guidance channels affects the quantity and origin of axons that regenerate after complete spinal cord transection, and can improve functional recovery. Determining the optimum matrices and growth factors for insertion into these guidance channels will improve regeneration of the injured spinal cord.

Keywords: Axonal regeneration; Methylcellulose; Matrigel™; Fibroblast growth factor-1; Neurotrophin-3; Functional recovery

*Corresponding author. Tel.: +416 978 1460; fax: +416 978 4317.
**Corresponding author. Tel.: +416 603 5889; fax: +416 603 5298.
E-mail addresses: molly@ecf.utoronto.ca (M.S. Shoichet), charles.tator@uhn.on.ca (C.H. Tator).

0142-9612/$ - see front matter © 2005 Elsevier Ltd. All rights reserved.
doi:10.1016/j.biomaterials.2005.07.025

1. Introduction

As our understanding of spinal cord regeneration advances, several regeneration and repair strategies have demonstrated improved outcome after spinal cord injury [1–3], and many of these strategies reflect the importance of a combination of strategies for optimum recovery. To achieve recovery it will be essential to understand the mechanisms underlying the repair so that the appropriate combination of strategies can be selected.

For example, in selecting the appropriate spinal cord injury repair model, it is important to differentiate between repair that promotes axonal collateralization and true axonal regeneration. The quality of a repair will be suboptimal when achieved by axonal branching or collateralization from an intact axon that has been spared from injury. In contrast, the repair would be optimal when achieved through true axonal regeneration from the axonal end of a transected or damaged axon. Ideally, all transected axons would regenerate rather than have spared axons compensate for lost function through collateralization. To differentiate between collateralization from axons spared from injury and true regeneration requires animal models of complete transection of the spinal cord rather than models of partial spinal cord injury. While partial injury models may be more relevant to the majority of human spinal cord injuries, and complete transection injuries to a minority of injuries, partial injury models do not allow precise differentiation between regeneration and collateralization.

While complete spinal cord transection models facilitate the differentiation between factors that stimulate regeneration and collateralization, complete transection models lack a cavity at the injury site making it difficult to apply many types of treatments. For example, administered growth factors, or transplanted cells are not easily contained at the injury site after complete cord transection. As well, the potentially extensive scarring from fibroblasts or astrocytes in complete transection models may inhibit axonal regeneration and prevent evaluation of a repair strategy.

To facilitate the delivery of a combination of factors to enhance repair and to decrease scarring in complete transection models, we and others have utilized the method of entubulation [4–9]. Utilizing a channel to contain regenerative factors allows their efficacy to be compared more uniformly because the channel allows the assessment of the regenerative factors in an environment that contains axons, glia, endothelial cells, inflammatory cells and fibroblasts. We have previously reported that a synthetic hydrogel channel composed of poly(2-hydroxyethyl methacrylate-*co*-methyl methacrylate) (pHEMA-MMA) implanted without a matrix after complete spinal cord transection facilitated motor axon regeneration from the brainstem [4]. In the present study, we examined whether the addition of a matrix and/or growth factor to the channel would improve axonal regeneration and if there was a difference between the matrices tested in terms of the quantity and types of axons that regenerated after complete spinal cord transection. We chose to compare the following matrices—fibrin, collagen, Matrigel^{TM} and methylcellulose—because each of fibrin [1,4,10,11], collagen [12,13], Matrigel^{TM} [5,14–18], and methylcellulose [12,19], have demonstrated regenerative capacity in the nervous system, and may improve regeneration through interactions with ligands present in the matrix. For example, fibronectin in fibrin, laminin in Matrigel, and collagen are all components of the extracellular matrix and are known to provide haptotatic cues to nerve fibers.

We chose to compare fibroblast growth factor-1 (FGF-1) and neurotrophin-3 (NT-3) because both have demonstrated beneficial effects on spinal cord regeneration [1,10,11,20–26]. These neurotrophic factors were added only to collagen and fibrin glue because these matrices have been extensively studied with respect to spinal cord injury repair [1,7,21,27–31]. This is the first study comparing these promising materials/growth factors in pHEMA-MMA channels, which themselves have regenerative capacity [4].

2. Methods

2.1. Channel and small tube fabrication

All chemicals for the fabrication of the channels were purchased from Aldrich (Milwaukee, WI). Water was distilled and deionized at 18 ΩM. Channels were synthesized by the liquid–liquid centrifugal casting technique previously described in detail by our group [32,33]. Briefly, the monomers, methyl methacrylate (MMA) and 2-hydroxyethyl methacrylate (HEMA), were dissolved in excess water in the wt ratios of 2.5:22.5:75, respectively. This mixture was stirred and degassed, then aqueous solutions of ammonium persulfate (APS) and sodium metabisulfite (SMBS) were added to reach a final concentration (with respect to the monomer) of 0.5 and 0.4 wt%, respectively. This solution was injected through rubber septa into a 15 cm length glass mold, with ID of 4.2 mm, which was then placed in the chuck of a horizontally mounted stirrer. Rotation commenced at 4700 rpm, as measured with a tachometer (Model 461893, Extech Instruments, Waltham, MA). As the monomer was polymerized, the polymer became insoluble in the aqueous solution and phase separated with unreacted HEMA monomer. This separated liquid phase is denser than water and pushed to the periphery of the glass mold by centrifugal forces. After approximately 5 h, the glass molds were removed from the horizontally mounted stirrers and the pHEMA-MMA hydrogel channels removed from the molds. The hydrogel channels were cut into 6 mm lengths and Soxhlet-extracted overnight in water.

Channels were individually packaged into cryovials with a punctured cap, and sterilized by autoclaving (20 min at 120 °C) prior to implantation.

Smaller tubes were also synthesized as one of the groups studied had 4 smaller tubes incorporated within the lumen of guidance channels (tubes within channels, TWC). These smaller tubes were manufactured using the same centrifugal casting process as above; however rubber septa-sealed capillary tubes with an inner diameter (ID) of 1.2 mm were used as a mold. In addition the tubes fabricated for inclusion within the channel had a different formulation than the nerve guidance channel. Ethylene glycol (EG) was included as a co-solvent, and the weight ratios of MMA, HEMA, EG and H_2O in the mixture were 5.77: 26.24: 18.36: 49.63, respectively. To this mixture, 10% APS and SMBS aqueous solutions were added to achieve a final concentration of 0.5 and 0.4 wt%, respectively, and these initiated the polymerization. The capillary tubes were then rotated horizontally at 6000 rpm for 5 h.

2.2. Characterization of channels and smaller tubes

Channels of 25 mm in length were extracted and sterilized as previously described, and mounted on a micro-mechanical tester (Dynatek Dalta, Scientific Instruments, USA) using barbed fitting and Luer Lok connectors. The hydrogel channels were pulled in tension at a rate of 1%/min, and changes in the load and distance measured. The elastic modulus calculated from the linear portion of the stress-strain curve represents the rigidity of the channels. The dimensions of the channels and tubes were measured after sterilization, using a stereomicroscope (Leica, MZ-6).

2.3. Animals and tracer materials

Adult, female Sprague Dawley rats (Charles River, St. Constant, Quebec, Canada, 200–500 g) were used for this investigation. Female rats were used because of the ease of the management of bladder expression, and the decreased incidence of urinary tract infections in females compared to males in SCI experiments. Fluoro-gold (FG) was obtained from Fluorochrome (Denver, CO, USA). The animal protocols were approved by the Animal Care Committee of the Research Institute of the University Health Network in accordance with policies established by the Canadian Council of Animal Care.

2.4. Matrix preparation

The matrices inserted into the channel and the total numbers of animals utilized in the study are shown in Table 1. Dilute concentrations of matrix were used. Matrigel (Becton & Dickinson Biosciences, Mississauga, ON) was used as received. Methylcellulose solutions (2 wt%) (A4M Methocel, Dow Chemical) were prepared at 2° C in phosphate buffered saline (PBS) according to the manufacturers instructions and then sterilized through filtration. Collagen (type I) matrices (Vitrogen, Cohesion Technologies Inc, Palo Alto, California) were prepared as previously described [13] and injected into the guidance channel. The collagen was diluted to a concentration of 1.28 mg/ml and then buffered to a pH of 7.4 under aseptic conditions and at temperatures near 0° C to prevent premature gelling. Growth factors were mixed with the collagen to reach the following concentrations: 10 μg/ml FGF-1 or 1 μg/ml NT-3 (Promega, Madison WI) (Table 1). Fibrin (Aventis Behring, Marburg, Germany) was used as received and was mixed during surgery as described in the following section. FGF-1 and NT-3 were separately included in the fibrinogen component of the fibrin to achieve an overall concentration of 10 μg/ml or 1 μg/ml, respectively. The concentration of FGF-1 was based upon previous studies [13] demonstrating efficacy in axonal regeneration in the peripheral nervous system utilizing similar hydrogel channels. The concentration of NT-3 was based on previous in vivo studies of the biological effects of neurotrophins [34–36].

2.5. Channel and matrix implantation and functional assessment

There were ten groups of rats of approximately $n = 8$ per group as shown in Table 1. Rats were anesthetized with 2% halothane with 1:2 nitrous oxide to oxygen and then received preoperative cefazolin (40 g) in 5 ml of normal saline subcutaneously. After the T7-9 laminae were removed, the dura was incised and a synthetic expanded polytetrafluoroethylene

Table 1
The experimental groups and the number of animals analyzed by histological analysis

Matrix with or without growth factor	Paraformaldehyde	Formalin	Electron Microscopy	Total
TWC	4	3	0	7
Collagen	3	3	2	8
Fibrin	3	3	2	8
Matrigel	3	3	2	8
Methylcellulose	3	3	2	8
Collagen + FGF-1	4	4	0	8
Collagen + NT-3	4	3	0	7
Fibrin + FGF-1	3	3	2	8
Fibrin + NT-3	4	3	1	8
Unfilled channel (control)	3	3	2	9
Transection (no channel) (negative control)	8	3	0	11

All animals underwent weekly BBB functional assessment for 8 weeks.

membrane (ePTFE; Preclude®, W. L. Gore & associates, Inc., Flagstaff, Arizona, USA) was sutured to one side of the durotomy with two 8-0 Ethilon sutures. With an operating microscope, the spinal cord at the T8 level and any nearby nerve roots were then transected with microscissors. The transection site was carefully examined under microscopy to ensure complete transection of the spinal cord and all spinal roots in the vicinity. Gelfoam (Pharmacia & Upjohn Inc., Mississauga, Ontario, Canada) was placed in the gap between the two stumps for hemostasis. After removal of the Gelfoam, there was usually a persisting gap of approximately 4 mm between the two stumps of the spinal cord. A pHEMA-MMA channel with or without growth factor or matrix was randomly chosen for placement between the two stumps. A small "V" was incised in the dorsal aspect of the channel at the rostral and caudal ends to facilitate stump insertion. A blunt hook was then placed under the cut rostral stump to elevate the stump and then to insert it into the channel, facilitated by the increased opening due to the v-cut. This was repeated for insertion of the caudal stump into the channel. Each stump was inserted approximately 1 mm into the ends of the channel leaving a gap of approximately 2–4 mm between the stumps.

Two 30 gauge tuberculin syringes filled with liquid matrix were then injected to fill the gap between the transected spinal cord stumps within the larger pHEMA-MMA channel (see Fig. 1). The total volume of matrix injected was approximately 0.1 ml. Care was taken to ensure there were no air bubbles within the channel lumen. For the fibrin matrix, fibrinogen and thrombin were injected simultaneously, resulting in a total injection volume of 0.1 ml. In another strategy, 4 smaller pHEMA-MMA tubes (<4 mm in length) were inserted into the larger channel (tubes within channels, TWC) prior to insertion of the caudal stump. The unfilled channel control group did not have matrix or growth factor injected into the channel. After matrix insertion was completed in all groups (see Table 1), fibrin glue (20 μl of fibrinogen and 20 μl of thrombin, Aventis Behring, Marburg, Germany) was then applied dorsally to the stump-channel interface at rostral and caudal ends (see Fig. 1). The synthetic dural membrane was then positioned such that it covered the channel-cord construct entirely. Negative controls (transection control) animals ($n = 8$) had the transection at T8, and the synthetic dural membrane was placed between the two stumps and positioned so that the rostral edge of the synthetic dural membrane was ventral to the rostral stump, and the caudal edge of the membrane was dorsal to the caudal stump. This step was taken to ensure that there would be no possibility of re-establishment of tissue continuity between the two cord stumps.

The wound was closed in layers with 3-0 Vicryl sutures (Johnson & Johnson, Peterborough, Ontario, Canada) in the paraspinal muscles and Michel clips (Fine Science Tools, North Vancouver, B.C., Canada) in the skin. Buprenorphine (0.03 mg/kg, subcutaneously) was given postoperatively and animals had their bladders expressed manually three times a day. Urinary tract infections were treated with ampicillin (125 mg every 12 h, subcutaneously) and gentamicin (2 mg once a day, subcutaneously) was added for urinary tract infections persisting more than 5 days.

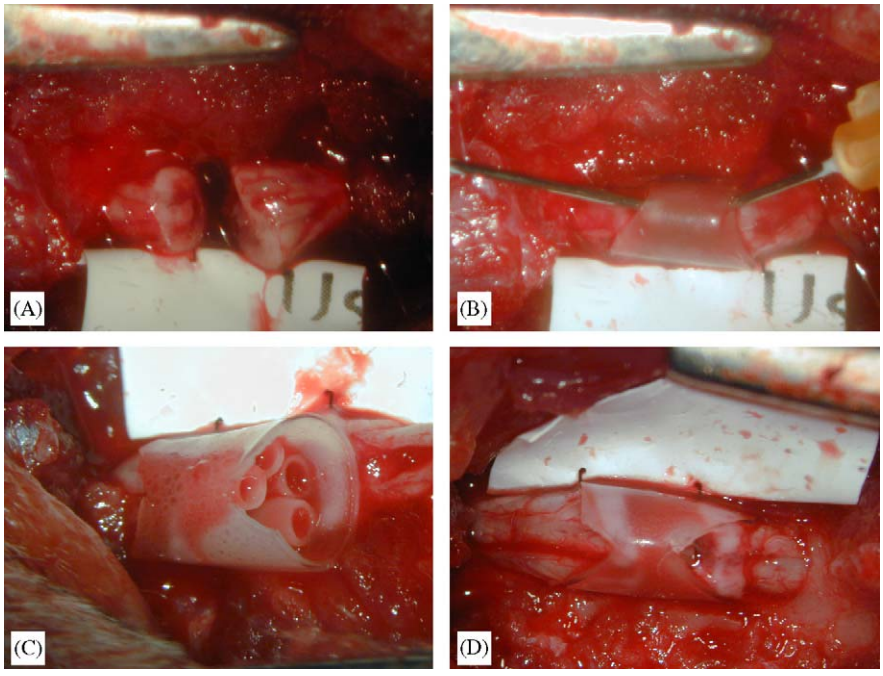

Fig. 1. (A) is an intraoperative photomicrograph demonstrating the spinal cord after complete cord transection. In (B), the two spinal cord stumps have been placed within the large channel and two 30 gauge tuberculin syringes filled with liquid matrix were used to fill the gap between the transected spinal cord stumps. (C) is an intraoperative photomicrograph showing the TWC construct prior to placement of the caudal stump into the larger channel. The proximal cord stump has already been inserted into the larger channel. For (A) and (B), the Preclude membrane duraplasty is seen at the bottom of the figure, and for (C) and (D), the duraplasty membrane is seen at the top of the figure. For all photomicrographs, rostral is to the left, and caudal is to the right. The outer diameter of the channels and smaller tubes are 4.19 ± 0.04 mm and 1.24 ± 0.03 mm, respectively.

Functional assessment was performed weekly with the Basso, Beattie, and Bresnahan (BBB) [37] scoring system, and all animals were videotaped while ambulating for 4 min just prior to tracer insertion or perfusion (described below). The period of observation was 8 weeks for all groups.

2.6. Retrograde axonal tracing and immunohistochemistry

The axonal tracer and immunohistochemical techniques were similar to those used in our previous report [38]. Briefly; Rats were anesthetised with 2% halothane with 1:2 nitrous oxide to oxygen. retrograde tracing with FG was performed in half the animals at each timepoint. After the predetermined period of observation, rats underwent laminectomy at T13 and complete spinal cord transection with microscissors. A pledget of gelfoam (0.5 mm^2) was soaked in a solution of FG in normal saline (4% for FG) and then placed in the transection site. Petroleum jelly (Sherwood Medical, St. Louis, Mo, USA) was then placed over the spinal cord and FG pledget at the laminectomy site. The muscles were closed with 3-0 Vicryl and the skin with Michel suture clips. After 7 days, the tissue was prepared as described below, and the cord and brain sections examined for evidence of retrograde labeling.

2.7. Tissue preparation

Animals were sacrificed at the end of the planned period of observation or 7 days later if FG was inserted. All animals were sacrificed by intraperitoneal injection of 0.7–1.0 ml of sodium pentobarbital (65 mg/ml). After thoracotomy they received an intracardiac injection of 1 ml of 1000 U/ml heparin, and then the animals with axonal tracing were perfused with 500 ml of 4% paraformaldehyde in 0.1 mM phosphate buffer (PB), and the rest of the animals were perfused with 500 ml of 10% neutral buffered formalin.

In animals with axonal tracers, the brain and spinal cord were removed, cryoprotected with 30% sucrose in PB (24 h, 4 °C), and then frozen and embedded in Optimum Cutting Temperature (OCT) compound (Stephens Scientific, Riverdale, New Jersey, USA). Coronal sections of the entire brain were cut in a cryostat at 40 μm, and serial parasagittal sections of the spinal cord encompassing the transection site (see Fig. 1) and the implanted channel were cut at 20 μm in a 1:7 series and mounted on cold (−20 °C) Superfrosted Plus slides (Fisher Scientific, Markham,Ontario, Canada).

It has been observed that animals with spinal cord transection show significant autofluorescence of cortical, brainstem and spinal neurons that interferes with identification of FG labeling. To eliminate this autofluorescence artifact, the brain sections were left to dry and selected sections treated for autofluorescence as described previously [38]. Briefly, the brain sections were washed in 0.1 M phosphate buffered saline (PBS), dipped in distilled water, and treated with 0.5% $CuSO_4$ (Sigma, St. Louis, MO, USA) in ammonium acetate buffer (50 mM, pH 5.0; Sigma, St. Louis, MO, USA) for 10 min, washed with distilled water or PBS, and then visualized in a hydrated state. Sections that dried prior to viewing were rehydrated with PBS.

Spinal cord sections were examined for FG using a fluorescent microscope and filter blocks as described below. Sections for immunohistochemistry were kept hydrated with PBS, photographed, and processed for immunohistochemistry.

For the formalin fixed animals, a 2 cm long cord segment that encompassed the transection site and channel was removed, photographed, and embedded in paraffin. Serial parasagittal sections 8 μm thick were cut in a 1:10 series and sections stained with hematoxylin and eosin, Luxol Fast Blue with hematoxylin and eosin, Masson's trichrome, Von Kossa silver stain for calcium, and Prussian blue for iron. Immunohistochemistry for NF200, GFAP, CSPG, and NG2 was performed on these formalin fixed sections as described below.

2.8. Immunohistochemistry

FG labeled tissue was examined for immunocytochemistry with the following monoclonal antibodies: mouse anti-neurofilament 200, phosphorylated and non-phosphorylated clone N52 (NF-200; 1:500, Sigma, St. Louis, MO, USA; [39]) to visualize neurons and axons; mouse anti-glial fibrillary acidic protein (GFAP; 1:200, Boehringer-Mannheim Chemicon, Temecula CA, USA; [40]) to visualize astrocytes and astrocytic scarring; and mouse anti-chondroitin sulfate clone CS-56 (CS56; 1:100, Sigma, St. Louis, MO, USA; [41] to visualize chondroitin sulphate proteoglycan. Polyclonal antibodies included: rabbit anti-calcitonin gene related peptide (CGRP; 1:3000, DiaSorin, Stillwater, MN; [42]) to identify sensory axons; rabbit anti-serotonin (5-HT; 1:10 000, DiaSorin, Stillwater, MN, USA; [42]) to identify serotonergic axons; and rabbit anti-NG2 chondroitin sulfate proteoglycan (NG2; 1:800, Chemicon, Temecula, CA; [43]) to identify oligodendendrocyte precursor cells.

2.9. Immunocytochemistry of paraformaldehyde fixed tissue

All sections were washed three times with PBS for 10 min, and then blocked for endogenous peroxidase and/or then for nonspecific antibody binding. Endogenous peroxidases were blocked with 1% hydrogen peroxide for 30 min for GFAP and NG2 labeling, and for 10 min for 5HT and CGRP. Non-specific antibody binding was blocked at room temperature (RT) for 1 h with the following: 10% heat inactivated goat serum (HIGS) in PBS containing 0.3% Triton X-100 for NF-200 and GFAP; 20% HIGS in PBS for NG2, 4% normal goat serum (NGS) in PBS containing 0.1% Triton X-100 for CS56. The primary antibodies were then applied to the sections and incubated overnight at 4 °C. All primary antibodies were diluted in blocking solutions with the exception of the following: 5-HT and CGRP were diluted in 0.3% Triton X-100 in PBS; and NG2 was diluted in PBS. Sections were then washed three times in PBS, and incubated with the secondary antibody, Alexa Fluor™ 488 goat anti-mouse and goat anti-rabbit IgG (H + L) conjugate highly cross-adsorbed (1:500 dilution in PBS; Molecular Probes, Eugene, OR, USA) was applied for 1 h at RT. Sections were mounted without coverslips and viewed hydrated with PBS using a fluorescent microscope as described below.

2.10. Immunocytochemistry of formalin fixed tissue

Formalin fixed sections were deparaffinized. All sections were blocked for endogenous peroxidase with 1% methanol peroxidase for 30 min, except for those stained for NF-200, GFAP, and CS56. To unmask antigen sites, selected sections of slides for NG2 were placed in a pressure cooker with citrate buffer (pH 6.0) and heated in a microwave oven (Kenmore Sears Canada Inc., Model 88952) for 35 min on high. After heating, slides remained in the microwave for an additional 30 min and were then rinsed with PBS twice. For NF-200, a solution of ethylenediaminotetraacetic acid (EDTA) in pH 8 buffer was heated in the microwave for 15 min on high power. The slides were then placed in the EDTA solution in the pressure cooker, which was placed in the microwave for 8 min on high power. After heating, the slides were left in the microwave for 20 min and then rinsed with PBS twice. All sections were blocked for nonspecific antibody binding as previously described. Monoclonal antibodies GFAP (1:200, Chemicon), NF 200 (1:400,Sigma), CS56 (1:50, Sigma) and the polyclonal antibody NG2 (1:250, Chemicon) were then applied and incubated overnight at 4 °C. The primary antibodies were diluted in blocking solutions, with the exception of NG2 which was diluted in PBS. The appropriate biotinylated secondary antibodies and avidin-biotin peroxidase complex (Vectostain Elite ABC Kit Standard, Vector Laboratories, Burlington, Ontario, Canada) were then added. Vector VIP (VIP, Vector Laboratories, Burlington, Ontario, Canada) was applied as the chromogen. Sections were coverslipped with Entellan (EM Science, Gibbstwon, NJ, USA) and visualized under a light microscope (Nikon Eclipse TE300, Nikon Mississauga, Ontario, Canada). In all of the immunocytochemistry procedures appropriate negative controls were made with the omission of the primary antibodies.

2.11. Visualization of retrograde axonal tracing and fluorescent immunocytochemistry

A fluorescent microscope (Nikon Eclipse TE300) was used for fluorescence histological examination with the following filter blocks: Tx Red (excitation filter 540–580 nm, dichroic mirror DM 595, barrier filter BA600-660); G-2A (excitation filter 510–560, dichroic mirror DM575, barrier filter BA590); B-2E (excitation filter 450–490, dichroic mirror DM 505, emission 520–560); and UV-2A (excitation filter 330–380, dichroic mirror DM 400, barrier filter BA420). Images were captured with an Optronics digital camera and the Bioquant Nova Prime for Windows 9x Version 6.50.10 MR.

2.12. Quantification of the density of NF-200 and CGRP nerve fibers

To quantify the density of NF-200 and CGRP axons that regenerated within the channel a modification of the technique reported by Guest et al. was utilized [9]. After immunohistochemical staining of serial sections of the tissue bridge within the channel with NF-200 or CGRP, sections were examined with the fluorescent camera and photographed as described above controlling for fluorescent light exposure. Adjacent sections stained for GFAP were used to identify the stumps [14,16] and to ensure that the area counted was regenerated tissue and not spinal cord stump. Images were then imported into Bioquant and a line was drawn along the dorsal-ventral aspect of the tissue bridge that was within the channel and contained the highest number of stained nerve fibers. The total number of fibers in contact with the drawn line was then counted, and the density of nerve fibers was calculated as the total number of nerve fibers divided by the length of the drawn line. At least 3 serial sections/animal were quantified.

2.13. Statistics

BBB scores were analyzed with Two Way Repeated Measures ANOVA and post-hoc analysis was performed using the Bonferroni method. Analysis was performed with SigmaStat for Windows Version 2.03 and Microsoft® Excel 2000, and graphs were drawn with SigmaPlot for Windows Version 4.01. All behavioral and histological evaluations were performed blindly without knowledge of treatment group.

3. Results

3.1. Nerve guidance channels and small tubes

The sterilized nerve guidance channels had an elastic modulus of 262.8 ± 13.0 kPa ($n = 4$, mean $\pm$ standard deviation) and an equilibrium water content of $43.2 \pm 1.1\%$ H_2O ($n = 4$). The physical dimensions of the channels were 4.19 ± 0.04 mm outer diameter (OD); 3.42 ± 0.09 mm ID, with a wall thickness of 386 ± 50 μm ($n = 10$). The smaller tubes inserted into the lumen of the channels were 1240 ± 30 μm OD; 790 ± 45 μm ID, with a wall thickness of 230 ± 35 μm ($n = 10$). Both the channel and smaller tube had similar wall morphologies consisting of a rough, spongy inner layer and a gel-like outer layer, as previously described in detail [32].

3.2. Matrix supplemented pHEMA-MMA channels improve axonal regeneration

The morphology of the nerve fibers within the channels was affected by the matrix used. We do not know whether this was due to the chemical content or the physical structure of the matrices. However, dilute concentrations of the matrices were used, and therefore, we feel that it is more likely that the chemical content accounted for the differences in morphology of the nerve fibers. The nerve fibers in the collagen group were less oriented in the rostral-caudal direction based on the finding that in the parasaggital sections, more axons were seen as circular profiles rather than linear profiles. In contrast, when methylcellulose was used as the matrix, the majority of fibers were in a rostral-caudal direction and the majority of the fibers were in a fascicular pattern compared with those in the TWC and

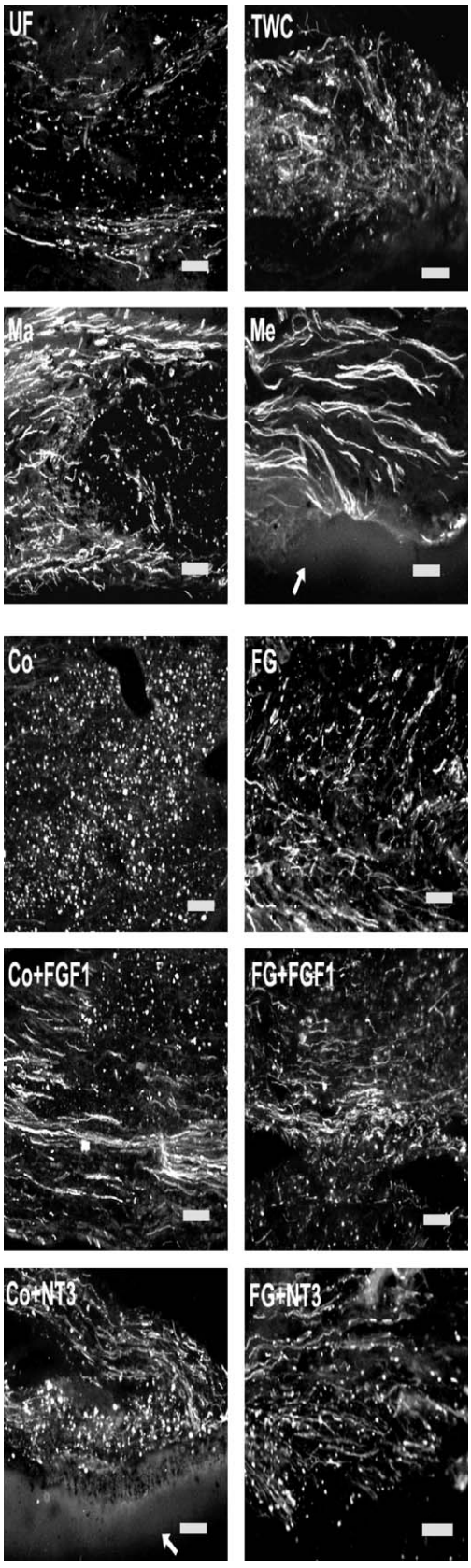

collagen groups (see Fig. 2). Indeed, the number of fibers oriented in the rostral-caudal direction was greatest with methylcellulose while TWC, fibrin and Matrigel™ showed an intermediate degree of rostral-caudal orientation. The collagen group had the least number of nerve fibers oriented in the rostral-caudal direction.

Interestingly, the addition of FGF-1 and NT-3 to collagen increased the orientation of the regenerating fibers in a rostral-caudal direction as fewer elongated axons were observed in cross section. Therefore, not only did the addition of FGF-1 and NT-3 to the collagen matrix increase the total density of nerve fibers, the rostral-caudal orientation of the fibers also increased. A similar increase in fiber orientation was not obvious for the fibrin-growth factor combinations (see Fig. 2).

The mean density of nerve fibers in the unfilled pHEMA-MMA channel was 12.7 ± 2.2 fibers/mm ($\pm$SEM). The addition of a matrix or a matrix plus a growth factor increased the density of nerve fibers within the channel compared to unfilled channel controls (see Fig. 3). The mean density of nerve fibers in TWC, collagen, fibrin, Matrigel™ and methylcellulose was 23.3 ± 3.9, 20.5 ± 3.7, 27.6 ± 3.1, 41.4 ± 3.0, and 36.3 ± 3.1 fibers/mm ($\pm$SEM), respectively (see Table 2). The mean density of NF-200 labeled fibers for fibrin, Matrigel™ and methylcellulose was significantly greater than in unfilled channel controls (one way ANOVA, $p < 0.001$).

The addition of FGF-1 or NT-3 to collagen significantly increased the mean density of nerve fibers to 31.6 ± 6.1 or 34.0 ± 4.5 fibers/mm ($\pm$SEM), respectively (one way ANOVA, $p = 0.001$) relative to that of collagen alone (20.5 ± 3.7 fibers/mm). In contrast, the addition of FGF-1 (23.7 ± 3.5) and NT-3 (27.3 ± 3.8) to the fibrin did not increase the mean density compared to fibrin alone (27.6 ± 3.1).

Fig. 2. Photomicrographs of parasagittal sections from the middle of the channels demonstrate the morphology of the regenerating fibers with the different matrices. Note that with all matrices there are regenerating NF-200 fibers present within the channels. Note that with methylcellulose, there are more linear fibers in a fascicular pattern than with the other matrices. Note that with the addition of neurotrophic factors to collagen, there are relatively fewer fibers in cross section compared to linear fibers. In contrast, the addition of neurotrophic factors to fibrin did not appear to significantly change fiber orientation. These sections were stained for NF-200 and visualized with a fluorescence microscope and all panels were taken at 100× magnification. Note that the channel wall (arrow) can be seen in some of the methylcellulose and collagen with NT3 photomicrographs. Scale bar = 100 μm. UF = unfilled channel, TWC = tubes within channels, Ma = Matrigel™, Me = methylcellulose, Co = collagen, FG = fibrin glue, Co + FGF1 = collagen with FGF1, FG + FGF1 = fibrin glue with FGF1, Co + NT3 = collagen with NT3, and FG + NT3 = fibrin glue with NT3).

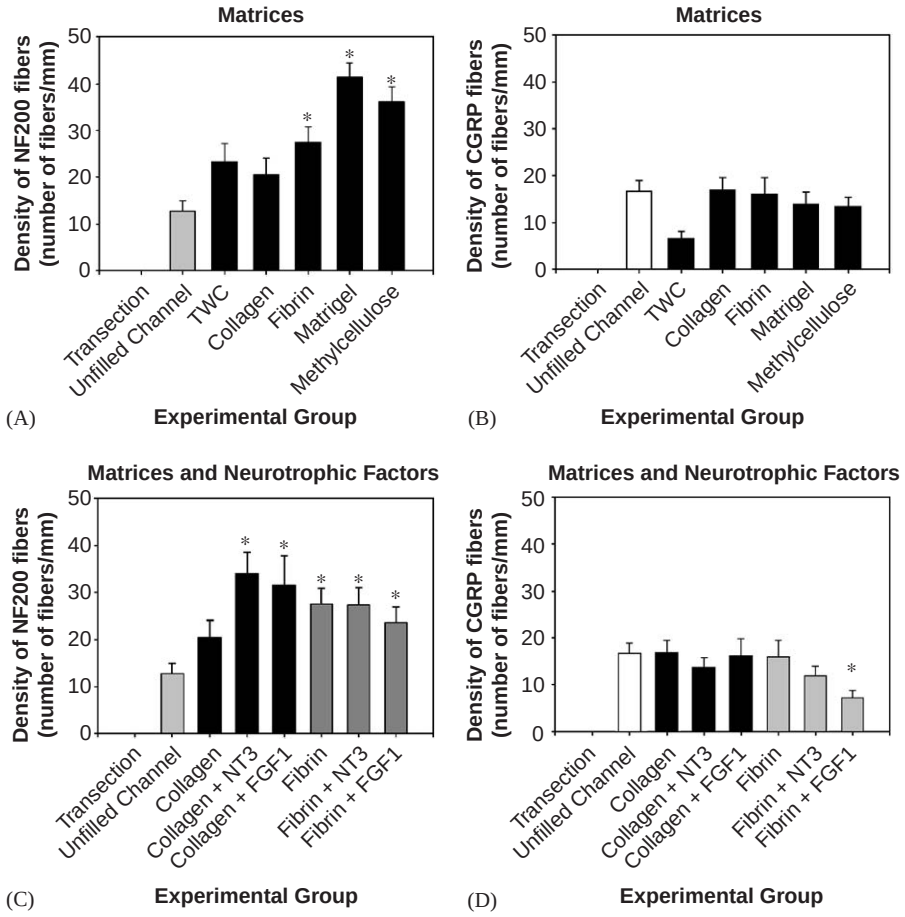

Fig. 3. Matrices and neurotrophic factors affect the density of NF-200 and CGRP axonal regeneration. (A) and (B) show the density of regenerated NF-200 and CGRP axons in the middle of the channel with different matrices, respectively. (C) and (D) show the density of regenerated NF-200 and CGRP axons with collagen or fibrin glue with and without the neurotrophic factors NT-3 or FGF-1. The mean NF-200 fiber density increased with the addition of different matrices and neurotrophic factors (bars with asterisks are significantly different compared to unfilled channel controls, $p<0.05$). Note that in the fibrin with FGF-1 group, the mean CGRP fiber density was significantly lower than the unfulfilled channel controls. Thus, the increase in the mean NF-200 fibers density and the lack of increase in mean CGRP fiber density suggests that other axonal tracts regenerated (see Table 2). Note that there were no regenerated fibers in the transection controls.

3.3. Matrix modification did not increase CGRP positive sensory axon regeneration

The mean CGRP fiber density in the unfilled channel controls was 16.7 ± 2.3 fibers/mm. There was no difference in the CGRP fiber density with the different matrices (one way ANOVA) suggesting that CGRP fiber regeneration is unaffected by the matrices used in this study. The addition of FGF-1 to fibrin, however, decreased the mean density of CGRP fibers compared to unfilled channel controls (one way ANOVA, $p<0.05$). Therefore, the increase in the density of NF-200 fibers was not due to an increase in the regeneration of CGRP fibers (see Table 2). Note that in the unfilled channel group, the percent of NF200 fibers that were not CGRP positive was a negative number. This can be attributed to the error associated with counting, and therefore, most, if not all, of the NF200 fibers in the unfilled channel group, could be accounted for by the regeneration of CGRP fibers. However, for the other experimental groups, there were NF200 fibers that could not be accounted for by CGRP regeneration. To better define these types of fibers that regenerated, we utilized retrograde axonal tracing to determine from which motor nuclei the axons regenerated.

We found that different matrices affected the source of motor axons that regenerated within the channels (see Fig. 4) as determined by retrograde tracing with FG. When unfilled channels were implanted, axons from the reticular, vestibular and raphe motor nuclei regenerated [4]. The addition of multiple smaller tubes into the lumen of the channel (i.e. TWC group), increased the total number of labeled brainstem neurons. However, there was an increase in the proportion of vestibular neurons, and a decrease in the number of raphe neurons that regenerated axons. With the collagen matrix, both vestibular and reticular neurons regenerated axons. With the fibrin matrix, there was an increase in the

Table 2
Nerve fiber density within the channels was compared for the different experimental nerve guidance channels tested (with matrices and growth factors) relative to controls

	Transection control	Unfilled channel	TWC	Matrigel	Methylcellulose	Collagen	Collagen + FGF1	Collagen + NT3	Fibrin glue	Fibrin glue + FGF1	Fibrin glue + NT3
Mean CGRP fiber density (#/mm ± SEM)	0.0 ± 0.0	16.7 ± 2.3	6.5 ± 1.5	13.8 ± 2.7	13.3 ± 2.1	16.9 ± 2.7	16.3 ± 3.5	13.8 ± 2.0	15.9 ± 3.7	7.2 ± 1.6	11.8 ± 2.2
Mean NF200 fiber density (#/mm ± SEM)	0.0 ± 0.0	12.7 ± 2.2	23.3 ± 3.9	41.4 ± 3.0	36.3 ± 3.1	20.5 ± 3.7	31.6 ± 6.1	34.0 ± 4.5	27.6 ± 3.1	23.7 ± 3.5	27.3 ± 3.8
% NF200 fibers that are CGRP positive	N/A	*	27.89	33.38	36.67	82.42	51.58	40.44	57.69	30.52	43.40
% NF200 fibers that are not CGRP positive	N/A	*	72.11	66.62	63.33	17.58	48.42	59.56	42.31	69.48	56.60

N/A = not applicable, note there were no regenerated fibers in the transection group, and therefore % NF200 fibers that are CGRP positive and % NF200 fibers that are not CGRP positive cannot be calculated.
SEM = standard error of the mean.
Nerve fibers stained for CGRP were distinguished from those stained for NF200.
*Since the axon counts exceed CGRP-labelled fibers, percentages cannot be calculated.

number of reticular neurons with regenerated axons, however, neither vestibular nor raphe axons regenerated. The inclusion of Matrigel™ did not allow any brainstem motor neurons to regenerate axons. The addition of a methylcellulose matrix within the pHEMA-MMA channels allowed reticular, vestibular and red nucleus (but not raphe) neurons to regenerate axons.

The addition of the neurotrophic factors also affected the type of brainstem motor neurons that regenerated axons. FGF-1 included with collagen increased the proportion of vestibular axon regeneration, but in contrast, NT-3 decreased the total number of brainstem motor neurons that regenerated axons, and appeared to permit only reticular axons to regenerate (Fig. 4). The inclusion of either FGF-1 or NT-3 within the fibrin matrix reduced the number of labeled brainstem neurons.

3.4. EM shows that myelination of regenerating axons occurs within the channel

Electron microscopy confirmed axonal regeneration and myelination within the channel. There also tended to be a laminated architecture to the regenerated tissue within the channel as shown in Fig. 5 with collagen surrounding the regenerating axons. Adjacent to the inner wall of the channel there were fibroblast-like cells, then collagen, then axons with varying degrees of myelination. Regenerating axons could also be found within the channel wall. Schwann cells may be responsible for the myelination observed (as observed in Fig. 5b) and may have migrated from the dorsal roots that were transected during laminectomy. Myelinating cells without a basal lamina could also be observed. These cells could represent regenerating Schwann cells that have not yet laid down a basal lamina or oligodendroglial cells. There was increased GFAP labeling closer to the transected stump tips both rostrally and caudally, yet minimal astrocytes were found within the channel itself.

3.5. Functional recovery

Several groups showed significant locomotor functional recovery as demonstrated by BBB scoring (see Figs. 6 and 7; two way repeated measures ANOVA, all pairwise multiple comparison procedures, Bonferroni *t*-test). At week 7, the fibrin, TWC and fibrin with FGF1 groups showed significant functional improvement compared to unfilled channel controls ($p = 0.001$, 0.014, and 0.010, respectively) and to transection controls ($p = 0.001$, 0.020, and 0.014, respectively). The TWC group had improved functional recovery compared to the collagen with FGF1 ($p = 0.022$), and collagen with NT3 groups ($p = 0.004$). The fibrin with FGF1 group had better functional recovery

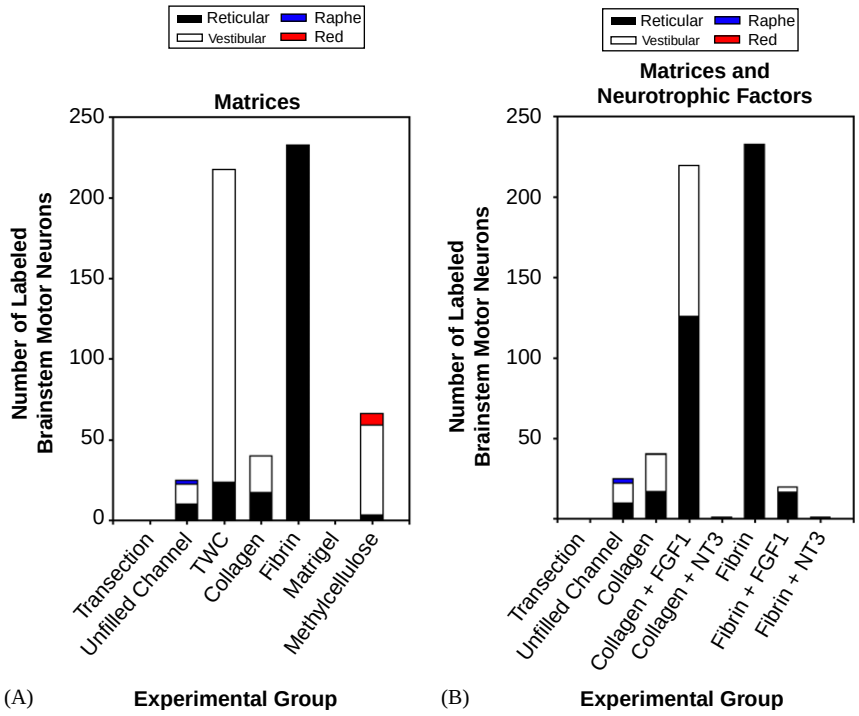

Fig. 4. Matrices and neurotrophic factors modify brain motor axon regeneration. The graphs demonstrate the number of fluoro-gold labeled brainstem neurons with the (A) different matrices and (B) neurotrophic factors. Note that the different matrices affect not only the total numbers of motor nuclei neurons that regenerated axons, but also the types of motor nuclei neurons that regenerated axons.

compared to the collagen with FGF1 group ($p = 0.036$) demonstrating the importance of matrix-growth factor combination for functional recovery.

At 8 weeks, however, only the fibrin and TWC groups showed a consistent improvement compared to transection controls ($p = 0.001$ and 0.003, respectively). The collagen group also showed improvement compared to transection controls ($p = 0.020$). In all but the collagen with FGF1 group, functional recovery appeared to plateau or even decrease at 8 weeks.

4. Discussion

In this study, we demonstrated that pHEMA-MMA hydrogel channels are capable of delivering combination therapies consisting of matrices and growth factors in a full transection injury model. Both the type of matrix and neurotrophic factor influence the quantity and types of axons that regenerate after full transection. Since there are often disparities between therapeutic strategies that affect axonal regeneration in vitro and in vivo, our channel can function as an "in vivo test tube" that contains the factors of interest, thereby allowing screening of several strategies in animal models of spinal cord injury repair.

The NF-200 fiber density outcome measure was helpful in determining the ability of the various matrices and growth factors and their combinations to support and enhance axonal regeneration in the synthetic channels. Fibrin, Matrigel™ and methylcellulose were approximately equally effective in significantly improving axonal regeneration within the channel compared with the unfilled channels. Inclusion of collagen matrix reduced the number of nerve fibers within the channel, which contrasts with what was observed in peripheral nerve guidance channels [12,13], yet similar to what others have observed in the CNS [44–47]. The mechanism accounting for reduced regeneration with collagen matrices in the spinal cord is not known. It has been suggested that the inability of injured CNS nerve fibers to regenerate into collagen may be related to the absence of an appropriate (astroglial) scaffolding structure and/or support system located within the collagen matrix [48].

Similarly, it is not clear why NT-3 and FGF-1 increased the number of regenerating axons in the presence of collagen, but not when combined with fibrin, except that if collagen is inhibitory, perhaps these growth factors overcome some of this inhibition. The combination of collagen and NT-3 appeared to have mainly increased local axonal regeneration or decreased long tract regeneration to the T13 level based on the paucity of brainstem neuronal labeling with retrograde FG at T13 produced by this combination. We and others have found that regeneration to at least the T13/L1 level is important for locomotor recovery after complete cord transection [31,49].

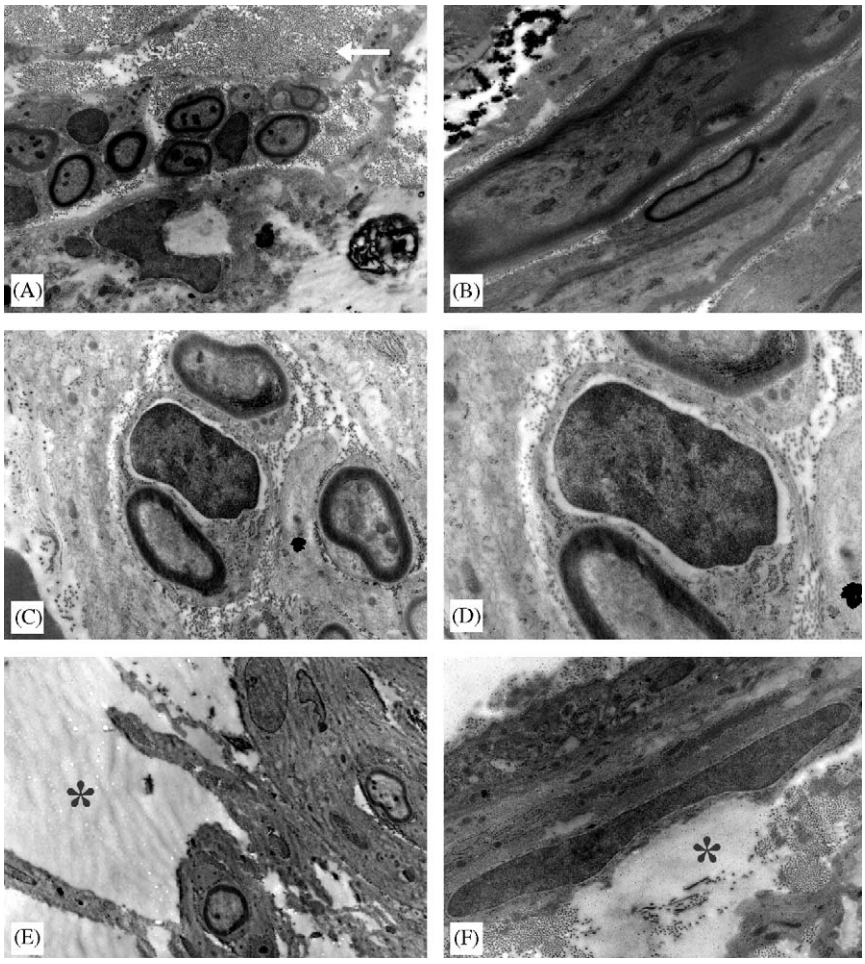

Fig. 5. Electron microscopy demonstrates regenerating axons present within the channel that have varying degrees of myelination (A). Note the numerous collagen fiber bundles present around these regenerating axons (arrow). Axons with varying degrees of myelination were also seen in longitudinal section within the channel (B) indicating that axons regenerated in different directions within the channel. Occasional cells were found to be myelinating more than one axon (C). Higher power view (D) of the myelinating cell in (C) demonstrates the lack of a basal lamina which suggests that these cells could represent either a regenerating Schwann cell that has not yet laid down a basal lamina or an oligodendroglial cell. (E) shows regenerating, myelinated axons within the channel wall (*). (F) shows a fibroblast next to the channel wall.

While several of the matrices that we tested have been previously shown to promote axonal regeneration within the spinal cord [1,4–6,11,14,16,18,46,50,51], this is the first study to determine that methylcellulose improved axonal regeneration within the spinal cord. By comparing the effect of the matrices on regeneration of CNS axons based on retrograde tracers, we found that of the matrices studied, only methylcellulose allowed regeneration of axons from the red nucleus. Our finding that Matrigel^{TM} alone did not allow regeneration of axons from any of the brainstem motor nuclei is consistent with the results of Bunge et al. [5,14,16,18].

The presence of CGRP fibers in the channels is probably due to axonal regeneration from local axons emanating mainly from CGRP containing neurons in nearby dorsal horns and dorsal root ganglia rather than from supraspinal neurons such as those in the brainstem. As such, increased regeneration of CGRP axons may be an undesirable local side-effect of any attempts to stimulate axonal regeneration. The undesirability may relate to an increase in pain or spasticity since increased CGRP in the injured spinal cord has been implicated in subserving central neurogenic pain after spinal cord injury [52–54].

Currently, there is no consensus as to what fiber tracts are necessary to obtain functional recovery, and the extent or length of axonal regeneration required. There are suggestions from the literature that the more tracts that are restored, the better the functional recovery [55], and that recovery can be obtained through axonal regeneration and restoration of interneuron networks. Others suggest that regeneration to a specific level (eg T13-L1), perhaps to stimulate the central pattern generator in the lumbar level, is required [31,49]. We found improvement in functional neurological recovery with the synthetic channels filled with matrices or growth factors compared with the unfilled channel and transection control groups. Only the fibrin and TWC

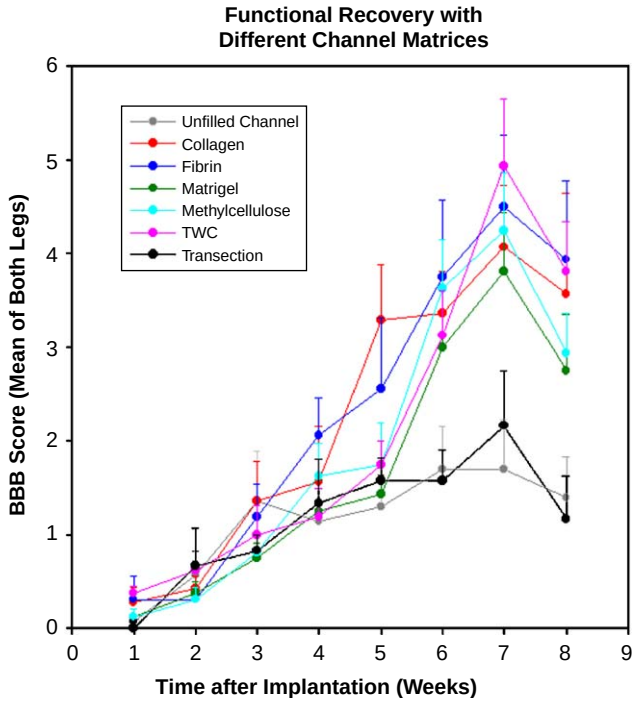

Fig. 6. Weekly mean BBB scores of animals with different matrices. Although there were higher BBB scores in the matrix groups than in the unfilled channel and transection controls, there were significant differences only at weeks 7 and 8.

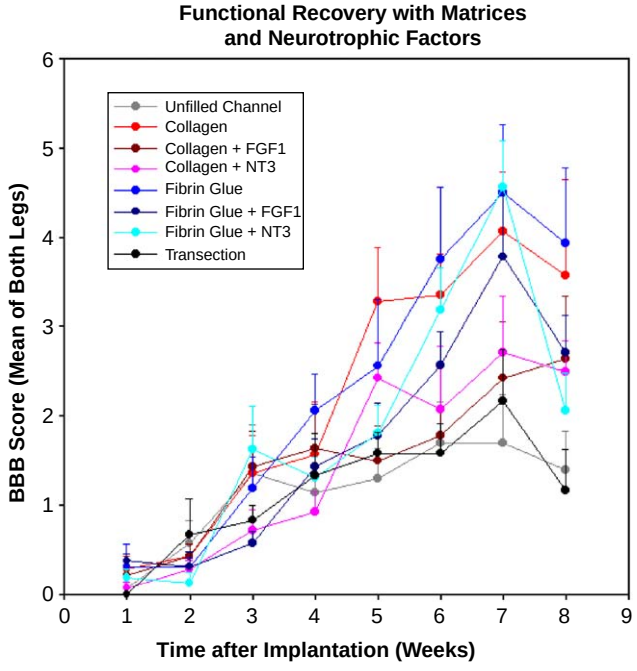

Fig. 7. Weekly mean BBB scores of animals with FGF-1 or NT-3 added to either fibrin or collagen. There were significant differences only at weeks 7 and 8.

groups showed a consistent improvement at both weeks 7 and 8 compared to transection controls. The functional improvement in the fibrin group may be due to the relatively increased number of axons regenerated from brainstem motor neurons and the increased regeneration of fibers at the repair site. While there was also a relatively increased number of axons that regenerated from brainstem motor neurons, the proportion of each type of neuron differed from the fibrin group in that there was more axonal regeneration from vestibular neurons. While there was no significant difference in the density of regenerated fibers at the transection site, there were proportionately fewer CGRP fibers present suggesting that other fiber types such as local interneuron type fibers may have regenerated and account for functional recovery. Thus, there may be different mechanisms of functional recovery obtained with the different repair strategies. Only through further study and testing will we be able to elucidate the mechanisms of recovery and perhaps learn to improve the extent of recovery.

The variable improvement in functional recovery observed might also be due to the variable rates of axonal regeneration that each matrix or neurotrophic factor promotes. For example, both the TWC and fibrin with FGF1 groups showed improvement in functional recovery compared to the collagen with FGF1 group at week 7, but not 8. Examination of the collagen with FGF1 groups demonstrated that while the majority of the other experimental groups showed a plateau or decline in functional recovery, the collagen with FGF1 groups continued to improve. Thus, collagen with FGF1 may be promoting the axonal regeneration of a subset of axons that regenerate at a different rate compared to those axons stimulated by other matrices with and without growth factors.

Further studies with prolonged study times may elucidate whether there is a plateau or decline in functional recovery at 8 weeks, and whether the decline or plateau may be due to an environmental factor. If there is a plateau, a controlled release strategy incorporated into the device design, of for example another neurotrophic factor released at 8 weeks, may promote further regeneration and recovery. Alternatively, a concentration gradient of neurotrophins may guide regeneration over longer distances, as has been observed in vitro [44,45], and enhance recovery. It should be noted that the methods of testing functional recovery were limited because of the relatively limited locomotor function, reflected by low BBB scores [56]. Most of the standard tests of functional recovery are insensitive in rats with BBB scores of these low values. As we advance our ability to improve functional recovery, we may be able to apply other tests of functional recovery and detect other aspects of functional recovery such as improved sensation and proprioception.

Despite the lack of BBB score differences between the matrix groups, the differences observed in the type of motor neuron axon regenerating may be useful in choosing a matrix to, for example, accompany cells

that are included in the channel. Other investigators have observed increased axonal regeneration when cells have been transplanted into the channels [5,9,44] or with cells alone [2,57]. The regenerative effects of cellular constructs may be greater with cell-matrix combinations.

It is unclear at present why one matrix may improve regeneration of one type of fiber over another. While this study was not designed to specifically assess the quantitative regenerative capacity of each matrix and growth factor on all motor and sensory axons, channels allow the determination of the optimal combination of factors that enable a specific population of motor tract axons to regenerate. We found that the addition of neurotrophic factors to collagen increased the mean density of nerve fibers, however, the different neurotrophic factors modified the types of axons that regenerated. For example, the addition of FGF1 to collagen increased axonal regeneration from reticular and vestibular brainstem motor neurons, while the addition of NT3 decreased axonal regeneration from these motor nuclei. In our study, methylcellulose was the only matrix that allowed regeneration from red nucleus neurons, and thus appears to be most promising. It would be of interest to determine whether the addition of neurotrophic factors to methylcellulose improves the quantity and the types of nerve fibers that regenerate. In our study, each combination of channel and matrix was tested as it is difficult to predict how the combination of factors will interact and which combination will be effective. Only through this type of detailed investigation can the effectiveness of specific combinations of factors be elucidated.

While the addition of cells to collagen [48,58], fibrin [21,30,31] and Matrigel [5,14,18] has been shown to improve regeneration, the effect of adding cells to methylcellulose in promoting axonal regeneration has not been studied and may hold promise in promoting axonal regeneration and functional recovery.

In addition, as most spinal cord injuries are not complete transections, the injury model may be modified to have the channels inserted into cavities associated with partial injuries for the regeneration of specific tracts. The TWC design is of interest as it may allow specific axons to regenerate in a spatial fashion, where each small tube contains a different regenerative therapy. A tube could be aligned to reapproximate specific tracts or to deliberately align a tract to a certain region that might improve axonal regeneration. An example would be to direct a tract away from inhibitory white matter toward more permissive gray matter. The TWC group also allowed us to test the concept that increasing the contact surface area is important for axonal regeneration. Using an increased number of smaller tubes allowed us to increase the contact surface area.

The quest for a cure for spinal cord injury has led many researchers to believe that there will be no single magic bullet. Rather, a combination of therapies will be required to not only improve axonal regeneration, but also to improve function. While the majority of strategies have been assessed with partial injury models, assessing the results has often been clouded by questions of whether true regeneration occurred or whether the visualized axons are from collateralization from intact axons spared from injury. Functional recovery in partial injury models also does not allow determination of whether recovery is due to regeneration of axons or due to plasticity of spared tracts. In contrast, the complete transection model used in the present study eliminates the uncertainties associated with partial injury models, and also allows testing of therapeutic agents contained within the channel, singly or in combination.

Acknowledgments

We thank the Natural Sciences and Engineering Research Council of Canada (MSS and CHT) and the Canadian Institutes of Health Research (ET) for funding. We are grateful to Peter Poon, Rita Van Bendegem, Lauren Lukas and Anand Govindarajan for histological analysis.

References

[1] Cheng H, Cao Y, Olson L. Spinal cord repair in adult paraplegic rats: partial restoration of hind limb function. Science 1996;273:510–3.

[2] Ramon-Cueto A, Cordero MI, Santos-Benito FF, Avila J. Functional recovery of paraplegic rats and motor axon regeneration in their spinal cords by olfactory ensheathing glia. Neuron 2000;25:425–35.

[3] Rapalino O, Lazarov-Spiegler O, Agranov E, Velan GJ, Yoles E, Fraidakis M, Solomon A, Gepstein R, Katz A, Belkin M, Hadani M, Schwartz M. Implantation of stimulated homologous macrophages results in partial recovery of paraplegic rats. Nat Med 1998;4:814–21.

[4] Tsai EC, Dalton PD, Shoichet MS, Tator CH. Synthetic hydrogel guidance channels facilitate regeneration of adult rat brainstem motor axons after complete spinal cord transection. J Neurotrauma 2004;21:789–804.

[5] Xu XM, Guenard V, Kleitman N, Bunge MB. Axonal regeneration into Schwann cell-seeded guidance channels grafted into transected adult rat spinal cord. J Comp Neurol 1995;351:145–60.

[6] Spilker MH, Yannas IV, Kostyk SK, Norregaard TV, Hsu HP, Spector M. The effects of tubulation on healing and scar formation after transection of the adult rat spinal cord. Restor Neurol Neurosci 2001;18:23–38.

[7] Spilker MH, Yannas IV, Hsu HP, Norregaard TV, Kostyk SK, Spector M. The effects of collagen-based implants on early healing of the adult rat spinal cord. Tissue Eng 1997;3:309–17.

[8] Oudega M, Gautier SE, Chapon P, Fragoso M, Bates ML, Parel JM, Bunge MB. Axonal regeneration into Schwann cell grafts within resorbable poly(alpha-hydroxyacid) guidance channels in the adult rat spinal cord. Biomaterials 2001;22:1125–36.

[9] Guest JD, Rao A, Olson L, Bunge MB, Bunge RP. The ability of human Schwann cell grafts to promote regeneration in the transected nude rat spinal cord. Exp Neurol 1997;148:502–22.
[10] Cheng H, Liao KK, Liao SF, Chuang TY, Shih YH. Spinal cord repair with acidic fibroblast growth factor as a treatment for a patient with chronic paraplegia. Spine 2004;29:E284–8.
[11] Levi AD, Dancausse H, Li X, Duncan S, Horkey L, Oliviera M. Peripheral nerve grafts promoting central nervous system regeneration after spinal cord injury in the primate. J Neurosurg Spine 2002;96:197–205.
[12] Wells MR, Kraus K, Batter DK, Blunt DG, Weremowitz J, Lynch SE, Antoniades HN, Hansson HA. Gel matrix vehicles for growth factor application in nerve gap injuries repaired with tubes: a comparison of biomatrix, collagen, and methylcellulose. Exp Neurol 1997;146:395–402.
[13] Midha R, Munro CA, Dalton PD, Tator CH, Shoichet MS. Growth factor enhancement of peripheral nerve regeneration through a novel synthetic hydrogel tube. J Neurosurg 2003;99:555–65.
[14] Chen A, Xu XM, Kleitman N, Bunge MB. Methylprednisolone administration improves axonal regeneration into Schwann cell grafts in transected adult rat thoracic spinal cord. Exp Neurol 1996;138:261–76.
[15] Guenard V, Kleitman N, Morrissey TK, Bunge RP, Aebischer P. Syngeneic Schwann cells derived from adult nerves seeded in semipermeable guidance channels enhance peripheral nerve regeneration. J Neurosci 1992;12:3310–20.
[16] Oudega M, Xu XM, Guenard V, Kleitman N, Bunge MB. A combination of insulin-like growth factor-I and platelet-derived growth factor enhances myelination but diminishes axonal regeneration into Schwann cell grafts in the adult rat spinal cord. Glia 1997;19:247–58.
[17] Pinzon A, Calancie B, Oudega M, Noga BR. Conduction of impulses by axons regenerated in a Schwann cell graft in the transected adult rat thoracic spinal cord. J Neurosci Res 2001;64:533–41.
[18] Xu XM, Chen A, Guenard V, Kleitman N, Bunge MB. Bridging Schwann cell transplants promote axonal regeneration from both the rostral and caudal stumps of transected adult rat spinal cord. J Neurocytol 1997;26:1–16.
[19] Tate MC, Shear DA, Hoffman SW, Stein DG, LaPlaca MC. Biocompatibility of methylcellulose-based constructs designed for intracerebral gelation following experimental traumatic brain injury. Biomaterials 2001;22:1113–23.
[20] Tuszynski MH, Peterson DA, Ray J, Baird A, Nakahara Y, Gage FH. Fibroblasts genetically modified to produce nerve growth factor induce robust neuritic ingrowth after grafting to the spinal cord. Exp Neurol 1994;126:1–14.
[21] Guest JD, Hesse D, Schnell L, Schwab ME, Bunge MB, Bunge RP. Influence of IN-1 antibody and acidic FGF-fibrin glue on the response of injured corticospinal tract axons to human Schwann cell grafts. J Neurosci Res 1997;50:888–905.
[22] Tuszynski MH, Weidner N, McCormack M, Miller I, Powell H, Conner J. Grafts of genetically modified Schwann cells to the spinal cord: survival, axon growth, and myelination. Cell Transplant 1998;7:187–96.
[23] Xu XM, Guenard V, Kleitman N, Aebischer P, Bunge MB. A combination of BDNF and NT-3 promotes supraspinal axonal regeneration into Schwann cell grafts in adult rat thoracic spinal cord. Exp Neurol 1995;134:261–72.
[24] Namiki J, Kojima A, Tator CH. Effect of brain-derived neurotrophic factor, nerve growth factor, and neurotrophin-3 on functional recovery and regeneration after spinal cord injury in adult rats. J Neurotrauma 2000;17:1219–31.
[25] Nakahara Y, Gage FH, Tuszynski MH. Grafts of fibroblasts genetically modified to secrete NGF, BDNF, NT-3, or basic FGF elicit differential responses in the adult spinal cord. Cell Transplant 1996;5:191–204.
[26] Schnell L, Schneider R, Kolbeck R, Barde YA, Schwab ME. Neurotrophin-3 enhances sprouting of corticospinal tract during development and after adult spinal cord lesion. Nature 1994;367:170–3.
[27] Chamberlain LJ, Yannas IV, Hsu HP, Strichartz G, Spector M. Collagen-GAG substrate enhances the quality of nerve regeneration through collagen tubes up to level of autograft. Exp Neurol 1998;154:315–29.
[28] Liu S, Said G, Tadie M. Regrowth of the rostral spinal axons into the caudal ventral roots through a collagen tube implanted into hemisected adult rat spinal cord. Neurosurgery 2001;49:143–50 (discussion 150–141).
[29] Marchand R, Woerly S, Bertrand L, Valdes N. Evaluation of two cross-linked collagen gels implanted in the transected spinal cord. Brain Res Bull 1993;30:415–22.
[30] Cheng H, Olson L. A new surgical technique that allows proximodistal regeneration of 5-HT fibers after complete transection of the rat spinal cord. Exp Neurol 1995;136:149–61.
[31] Tsai EC, Krassioukov AV, Tator CH. Corticospinal Regeneration Into Lumbar Grey Matter Correlates with Locomotor Recovery after Complete Spinal Cord Transection and Repair With Peripheral Nerve Grafts, Fibroblast Growth Factor 1, Fibrin Glue, and Spinal Fusion. J Neuropathol Exp Neurol 2005;64:230–44.
[32] Dalton PD, Flynn L, Shoichet MS. Manufacture of poly (2-hydroxyethyl methacrylate-*co*-methyl methacrylate) hydrogel tubes for use as nerve guidance channels. Biomaterials 2002;23:3843–51.
[33] Dalton PD, Shoichet MS. Creating porous tubes by centrifugal forces for soft tissue application. Biomaterials 2001;22:2661–9.
[34] Bregman BS, McAtee M, Dai HN, Kuhn PL. Neurotrophic factors increase axonal growth after spinal cord injury and transplantation in the adult rat. Exp Neurol 1997;148: 475–94.
[35] Diener PS, Bregman BS. Neurotrophic factors prevent the death of CNS neurons after spinal cord lesions in newborn rats. Neuroreport 1994;5:1913–7.
[36] Giehl KM, Tetzlaff W. BDNF and NT-3, but not NGF, prevent axotomy-induced death of rat corticospinal neurons in vivo. Eur J Neurosci 1996;8:1167–75.
[37] Basso DM, Beattie MS, Bresnahan JC. A sensitive and reliable locomotor rating scale for open field testing in rats. J Neurotrauma 1995;12:1–21.
[38] Tsai EC, van Bendegem RL, Hwang SW, Tator CH. A novel method for simultaneous anterograde and retrograde labeling of spinal cord motor tracts in the same animal. J Histochem Cytochem 2001;49:1111–22.
[39] Schumacher PA, Eubanks JH, Fehlings MG. Increased calpain I-mediated proteolysis, and preferential loss of dephosphorylated NF200, following traumatic spinal cord injury. Neuroscience 1999;91:733–44.
[40] Agrawal SK, Theriault E, Fehlings MG. Role of group I metabotropic glutamate receptors in traumatic spinal cord white matter injury. J Neurotrauma 1998;15:929–41.
[41] Fitch MT, Doller C, Combs CK, Landreth GE, Silver J. Cellular and molecular mechanisms of glial scarring and progressive cavitation: in vivo and in vitro analysis of inflammation-induced secondary injury after CNS trauma. J Neurosci 1999;19:8182–98.
[42] Brook GA, Plate D, Franzen R, Martin D, Moonen G, Schoenen J, Schmitt AB, Noth J, Nacimiento W. Spontaneous longitudinally orientated axonal regeneration is associated with the Schwann cell framework within the lesion site following spinal cord compression injury of the rat. J Neurosci Res 1998;53:51–65.

[43] Levine JM, Nishiyama A. The NG2 chondroitin sulfate proteoglycan: a multifunctional proteoglycan associated with immature cells. Perspect Dev Neurobiol 1996;3:245–59.
[44] Bunge MB. Transplantation of purified populations of Schwann cells into lesioned adult rat spinal cord. J Neurol 1994;242: S36–9.
[45] Joosten EA, Bar PR, Gispen WH. Collagen implants and corticospinal axonal growth after mid-thoracic spinal cord lesion in the adult rat. J Neurosci Res 1995;41:481–90.
[46] Houweling DA, Lankhorst AJ, Gispen WH, Bar PR, Joosten EA. Collagen containing neurotrophin-3 (NT-3) attracts regrowing injured corticospinal axons in the adult rat spinal cord and promotes partial functional recovery. Exp Neurol 1998;153: 49–59.
[47] Houweling DA, van Asseldonk JT, Lankhorst AJ, Hamers FP, Martin D, Bar PR, Joosten EA. Local application of collagen containing brain-derived neurotrophic factor decreases the loss of function after spinal cord injury in the adult rat. Neurosci Lett 1998;251:193–6.
[48] Joosten EA, Veldhuis WB, Hamers FP. Collagen containing neonatal astrocytes stimulates regrowth of injured fibers and promotes modest locomotor recovery after spinal cord injury. J Neurosci Res 2004;77:127–42.
[49] Ribotta MG, Provencher J, Feraboli-Lohnherr D, Rossignol S, Privat A, Orsal D. Activation of locomotion in adult chronic spinal rats is achieved by transplantation of embryonic raphe cells reinnervating a precise lumbar level. J Neurosci 2000;20:5144–52.
[50] Yoshii S, Oka M, Shima M, Taniguchi A, Taki Y, Akagi M. Restoration of function after spinal cord transection using a collagen bridge. J Biomed Mater Res 2004;70A:569–75.
[51] Iseda T, Nishio T, Kawaguchi S, Kawasaki T, Wakisaka S. Spontaneous regeneration of the corticospinal tract after transection in young rats: collagen type IV deposition and astrocytic scar in the lesion site are not the cause but the effect of failure of regeneration. J Comp Neurol 2003;464:343–55.
[52] Ondarza AB, Ye Z, Hulsebosch CE. Direct evidence of primary afferent sprouting in distant segments following spinal cord injury in the rat: colocalization of GAP-43 and CGRP. Exp Neurol 2003;184:373–80.
[53] Bennett AD, Chastain KM, Hulsebosch CE. Alleviation of mechanical and thermal allodynia by CGRP(8-37) in a rodent model of chronic central pain. Pain 2000;86:163–75.
[54] Christensen MD, Hulsebosch CE. Spinal cord injury and anti-NGF treatment results in changes in CGRP density and distribution in the dorsal horn in the rat. Exp Neurol 1997;147:463–75.
[55] Hase T, Kawaguchi S, Hayashi H, Nishio T, Mizoguchi A, Nakamura T. Spinal cord repair in neonatal rats: a correlation between axonal regeneration and functional recovery. Eur J Neurosci 2002;15:969–74.
[56] Metz GA, Merkler D, Dietz V, Schwab ME, Fouad K. Efficient testing of motor function in spinal cord injured rats. Brain Res 2000;883:165–77.
[57] Garcia-Alias G, Lopez-Vales R, Fores J, Navarro X, Verdu E. Acute transplantation of olfactory ensheathing cells or Schwann cells promotes recovery after spinal cord injury in the rat. J Neurosci Res 2004;75:632–41.
[58] Paino CL, Bunge MB. Induction of axon growth into Schwann cell implants grafted into lesioned adult rat spinal cord. Exp Neurol 1991;114:254–7.